

PREPARATION AND CHARACTERIZATION OF HMSPP/MMT/SILVER NANOCOMPOSITE FILMS WITH ANTIBACTERIAL ACTIVITY

^{1*}Washington Luiz Oliani, ¹Luiz Gustavo Hiroki Komatsu, ¹Isabelle Berenguer,
^{2,3}Nilton Lincopan, ⁴Vijaya Kumar Rangari, ¹Ademar Benevolo Lugao, ¹Duclerc
Fernandes Parra

¹Nuclear and Energy Research Institute, IPEN-CNEN/SP, Av. Prof. Lineu Prestes, 2242, Cidade Universitária,
CEP 05508-000, São Paulo – SP, Brazil

* washoliani@usp.br

²Department of Microbiology, Institute of Biomedical Sciences, University of Sao Paulo, Av. Professor Lineu
Prestes, 1374, CEP 05508-000, São Paulo, Brazil

³Department of Clinical Analysis, School of Pharmacy, University of Sao Paulo, São Paulo, Brazil

⁴Center For Advanced Materials Science and Engineering Tuskegee University, AL 36088, USA.

ABSTRACT

The aim of study was to use nanocomposites for bactericide packing for food. The polypropylene modified by irradiation in acetylene at dose of 12.5 kGy, also known as high-melt-strength-polypropylene (HMSPP), with montmorillonite (MMT) and silver nanoparticles (AgNPs) composed a mix to process by melt intercalation in a twin-screw extruder. As compatibilizer agent it has been used a propylene graft maleic anhydride copolymer (PP-g-MA). The nanocomposites were evaluated by Fourier Transformed Infrared Spectroscopy (FTIR), Differential Scanning Calorimetry (DSC), X-Ray Diffraction (XRD), Scanning Electron Microscopy (SEM), Energy Dispersive Spectroscopy (EDX) and determination of antibacterial activity. The results indicate the formation of microstructures predominantly intercalated and flocculated. Further, the antibacterial properties of the films were investigated against *Escherichia coli* (Gram-negative) and *Staphylococcus aureus* (Gram-positive) bacteria.

1. INTRODUCTION

Isotactic polypropylene (iPP) is a versatile thermoplastic polymer, one of the most widespread commodities due to its low price, and balanced properties. It is nontoxic, nonallergenic, chemically inert, and recyclable with a relatively low melting point [1]. The melt strength and viscosity of polypropylene (PP) decreases rapidly as the temperature rises over its melting point. High melt strength is very important for thermoforming, extrusion coating, blow molding, and foaming processes, etc. In this sense grafting by long chain branches onto PP backbone is a well-established technique to improve the melt strength of PP [2,3]. Branches are introduced into linear polypropylene (PP) to produce *high melt strength polypropylene* (HMSPP) with enhanced processability [4,5].

The development of organic/inorganic polymer nanocomposites has emerged as a research activity resulting in new applications of polymers for the great benefit of various industries.

Polymer compounds containing functional inorganic nanoparticles have demonstrated significant improvements in mechanical, thermal, electrical, and bactericidal properties [6]. Besides, antimicrobial surfaces implication in a range of infrastructure including hospitals, childcare centres, nursing homes, etc., to assist in minimizing the spread of disease and reducing the prevalence of illness and discomfort. Nosocomial infections (hospital-acquired infection) cases have increased rapidly in recent decades, and the prevalence of antibiotic-resistant pathogens is of particular concerns particularly to difficulties in treatment of patients to avoid high mortality rates [7]. The high performance of nanocomposite materials depends on the structure in nanosized dimensions and the homogeneous dispersion of nanoparticles within a polymer matrix. However, the fine dispersion of nanoparticles in a polymer using conventional compounding techniques is very difficult due to strong tendency of particles agglomeration [6,8].

The use of silver metal nanoparticles received greatest attention in comparison with other similar metals. Silver is relatively less toxic to human cells, albeit at very low concentrations. Concerning the mechanism of the antimicrobial activity of silver, is not completely understood. Studies have shown that the positive charge on the silver ion is critical for antimicrobial activity. The negative charge of the bacterial cell membrane imposes attraction to positively charged nanoparticles [9].

The conventional twin screw extrusion methods historically have been limited in successfully producing polymer nanocomposites with nonpolar polyolefins (e.g., polyethylene and polypropylene) [10,11], because high levels of filler exfoliation and dispersion are not typically achieved in the polymer matrix containing clay. Recent studies have explored modified and/or assisted twin screw extrusion setups, incorporating techniques such as ultrasonic irradiation [12,13] and sonication [14], with the intent of effectively mass-producing polymer nanocomposites with the desired morphology.

Several polymeric materials with different molecular weight such as polyethylene glycol (PEG), polyvinyl alcohol (PVA), poly(N-vinyl-2-pyrrolidone) (PVP), and others, mainly water soluble, have been used as coatings of silver nanoparticles to enable particle dispersion [15], and silver nanoparticles stabilized with oleic acid (AO) showed clear advantages in antibacterial activity, penetration bacteria cells, cytotoxicity, time effectiveness, efficiency, and stability against light [16]. Fig. 1 shows the structural formula of some surfactants used in polymers.

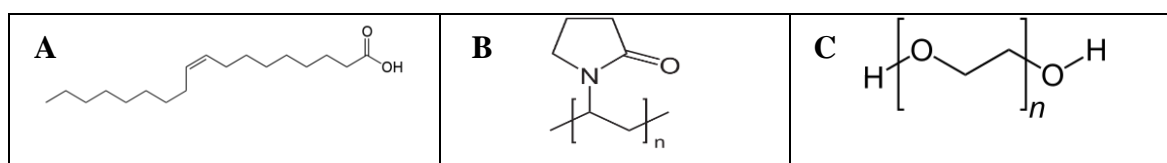


Figure 1: Structural formula of the main surfactants (A) Oleic acid (AO), (B) Polyvinyl pyrrolidone (PVP) and (C) Polyethylene glycol (PEG).

The aim of this work is to produce nanocomposite films polypropylene through the extrusion process, characterize these films and assess biocide activity.

2. EXPERIMENTAL

2.1. Materials

iPP with a melt flow index (MFI) of 1.5 dg min^{-1} and a weight average molecular weight of 338,000 g mol^{-1} Braskem (Brazil) was provided in the form of pellets. The polypropylene pellets were placed in a nylon container with acetylene (99.8%, White Martins). The irradiation process of the plastic container was carried out at room temperature and at a dose rate of 5 kGy h^{-1} , using a multipurpose ^{60}Co gamma irradiator. The dose used was 12.5 kGy monitored by a Harwell Red Perspex 4034 dosimeter. After irradiation, the pellets were submitted to heat treatment at $90 \text{ }^\circ\text{C}$ for 1 h to promote the recombination and termination reactions of the radicals, (HMSPP) [17,18]. These samples were irradiated in Center for Radiation Technology (CTR) of the Institute for Energy and Nuclear Research (IPEN-CNEN/SP).

The oleic acid (AO) was purchased from Labsynth (São Paulo-Brazil), average molecular weight $282,460 \text{ g mol}^{-1}$, and density: 0.895 g mL^{-1} , which acted as a surfactant for the AgNPs. Silver nanoparticles (AgNPs) were purchased from Sigma Aldrich. The commercial nanoclay Cloisite 20 was provided by BYK Additives Company; IRGANOX B 215 ED by Ciba and compatibilizer agent and propylene maleic anhydride graft copolymer (PP-g-MA) was supplied by Addivant (Polybond 3200).

Two different formulations containing the polypropylene were prepared and are represented in Table 1.

Table 1: Composition of constituents of polypropylene nanocomposites (wt%).

Samples	Matrix	Dose/kGy	PP-g-MA	Irganox	Cloisite	AgNPs	AO
PP1	HMSPP	12.5	-	2	-	-	-
PP2	HMSPP	12.5	2	2	3	0.25	10

2.2. Preparations of the PP-MMT-AgNPs Nanocomposite Films

The HMSPP 12.5 kGy in pellet was mixed with Irganox B 215 ED and PP-g-MA in a rotary mixer and maintained under this condition for 24 hours. Then the mixture was processed with the addition of clay (MMT 3% by weight) and silver nanoparticles (AgNPs 0.25% by weight) in a twin-screw extruder Haake co-rotating, model Rheomex PTW 16/25, Fig. 2, with the following processing conditions: the temperature profile (feed to die) was $175\text{-}230 \text{ }^\circ\text{C}$, with a speed of 100 rpm. After processed, the nanocomposites were granulated in a granulator Primotécnica W-702-3. The PP/MMT-AgNPs films were produced in planar sheet extruder and the material was placed directly into the hopper of the extruder with a temperature profile (feed to die) of $175\text{-}220 \text{ }^\circ\text{C}$, screw speed of 20 rpm and torque of 31-40 Nm. The films were produced with a thickness of $\sim 0.05 \text{ mm}$. A Unique ultrasound equipment model USC-1400, with a working frequency of 40 kHz and maximum intensity output of 135 watts, It was used to deagglomerate the silver nanoparticles solution with oleic acid.

Fig.2 shows the production of polypropylene films with nanosilver via extrusion processing.



Figure 2: Extruder Haake-Rheomex device used to process the polymeric films. Polymer Laboratory at Center for Chemical and Environmental Technology (CQMA) / Nuclear and Energy Research Institute (IPEN).

2.3. Methods

2.3.1. Scanning electron microscopy and dispersive spectroscopy

Scanning electron microscopy was done using an EDAX PHILIPS XL 30. In this project, thin coat of carbon was sputter coated onto the samples.

2.3.2. Fourier transformed infrared spectroscopy

The analyses were performed using attenuation total reflectance accessory (ATR) transmittance in the Thermo Nicolet spectrophotometer, model 380 FT-IR.

2.3.3. Differential scanning calorimetry

Thermal properties of specimens were analyzed using a differential scanning calorimeter DSC 822, Mettler Toledo. The thermal behavior of films was obtained by (1) heating from 25 to 280 °C at a heating rate of 10 °C min⁻¹ under nitrogen atmosphere; (2) holding for 5 min at 280 °C; and (3) then cooling to 25 °C and reheating to 280 °C at 10 °C min⁻¹.

2.3.4. X-ray diffraction

X-ray diffraction measurements were carried out in the reflection mode on a Rigaku diffractometer Mini Flex II (Tokyo, Japan) operated at 30 kV voltage and current of 15 mA with CuK α radiation ($\lambda = 1,541841 \text{ \AA}$).

2.3.5. Determination of antibacterial activity

An aliquot (400 μL) of a cell suspension of either *Staphylococcus aureus* ATCC 27853 (10^6 cells mL⁻¹) or *Escherichia coli* ATCC 25922 (10^6 cells mL⁻¹) prepared using the method described in JIS Z 2801[19] were held in intimate contact with each of the 2 replicates of the test surfaces supplied using a 45 x 45 mm² polypropylene film for 24 hours at 37 °C under humid conditions. The size of the surviving population was determined using a method based on JIS Z 2801. The viable cells in the suspension were enumerated by viable cell counts on MacConkey Agar after incubation at 37 °C for 24 hours using a 100 μL sample taken from the test surfaces.

3. RESULTS AND DISCUSSION

3.1. Scanning electron microscopy and dispersive spectroscopy

The SEM-EDX results are shown in Fig.3.

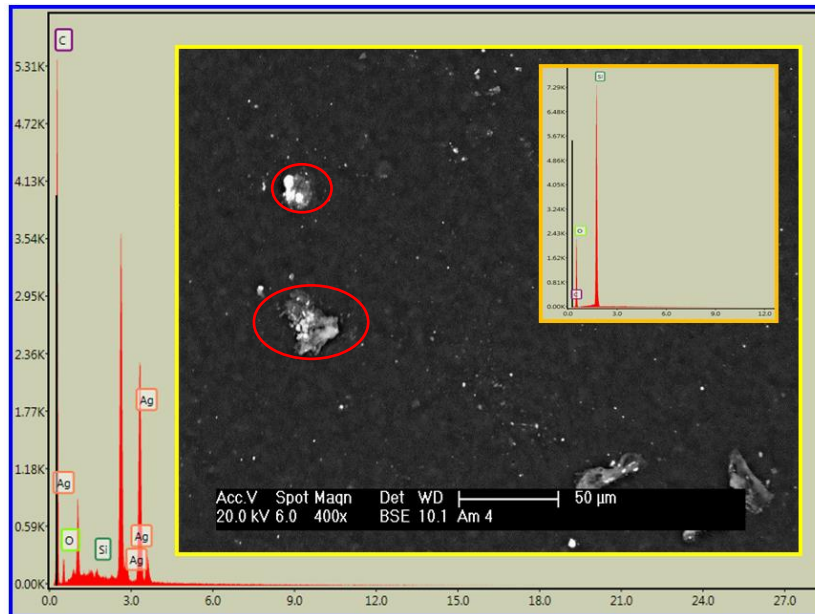


Figure 3: SEM micrograph and EDX of nanocomposite PP2 film.

The polypropylene nanocomposite film, Fig.3, there is a micrometer agglomerated/aggregates clay and the incidence of nanosilver, characterized by EDX. Larger particles (encircled) were observed which can be attributed to inhomogeneous dispersion of clay particles in PP matrix due to their inherent incompatibility (mix).

3.2. Fourier Transformed Infrared Spectroscopy

Fig. 4 presents the FTIR spectra of the polypropylene films with silver nanoparticles, oleic acid, and Cloisite nanoclay.

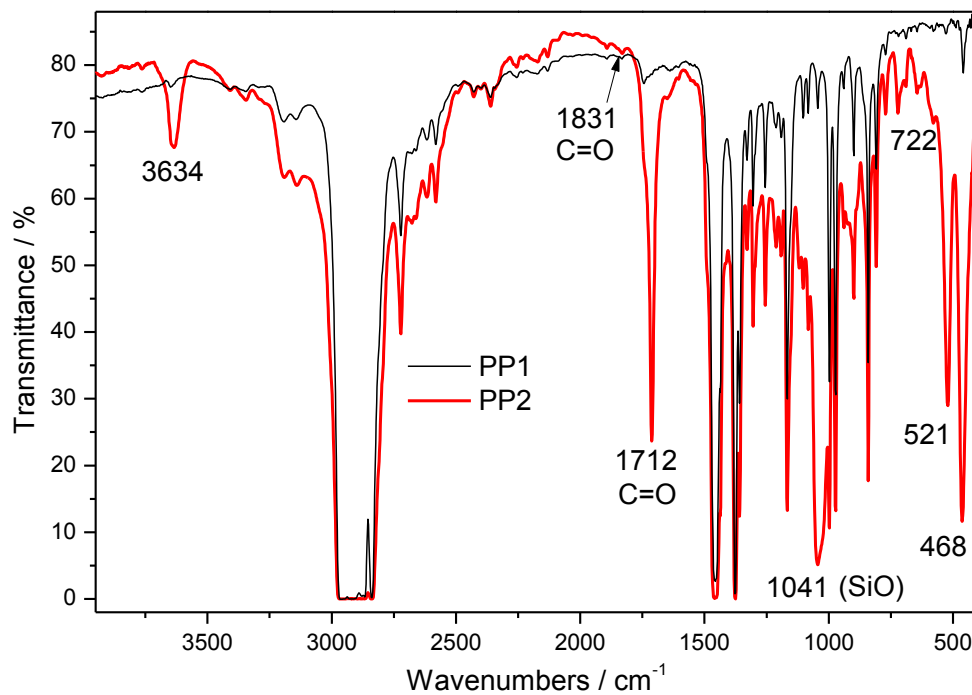


Figure 4: FTIR-ATR spectra of samples (PP1) film polypropylene HMSPP 12.5 kGy; and sample (PP2) nanocomposites HMSPP 12.5 kGy film with oleic acid.

In the nanocomposite samples a band at 3634 cm^{-1} related to the OH of the Al-OH and Si-OH a band at 1041 cm^{-1} and 468 attributed to the Si-O group of the clay can also be seen [20-22]. The strong peak located at 1712 cm^{-1} was due to the stretching of C=O characteristic peaks of a -COOH functional group [23,24] and absorption band with a peak at 1831 cm^{-1} is associated to the asymmetric stretching of the carbonyl of the maleic anhydride, according to [25]. The peak at 722 cm^{-1} was attributed to the C-H bending vibration of HC=CH links [26] and peak at 521 cm^{-1} was attributed to the Si-O-Al vibration [22,27]. According to FTIR spectra the polypropylene film with silver and nanoclay (PP2) shows Si-OH a band at 1041 cm^{-1} and 468 attributed to the Si-O group of the clay (Cloisite) and from C = O in 1712 cm^{-1} derived from oleic acid surfactant.

3.3. Differential scanning calorimetry

The DSC results are shown in Table 1 and Fig.5.

Table 1: DSC parameters for various polypropylene PP1 and PP2.

Samples	Melting peak temperature, T_{m1} /°C ($\pm 0.1\%$)	Crystallization peak temperature, T_C /°C ($\pm 0.1\%$)	Melting peak temperature, T_{m2} /°C ($\pm 0.1\%$)	Degree of crystallinity, X_C /% ($\pm 0.5\%$)
PP1	164.6	127.8	163.6	48.4
PP2	161.9	127.5	163.1	40.8

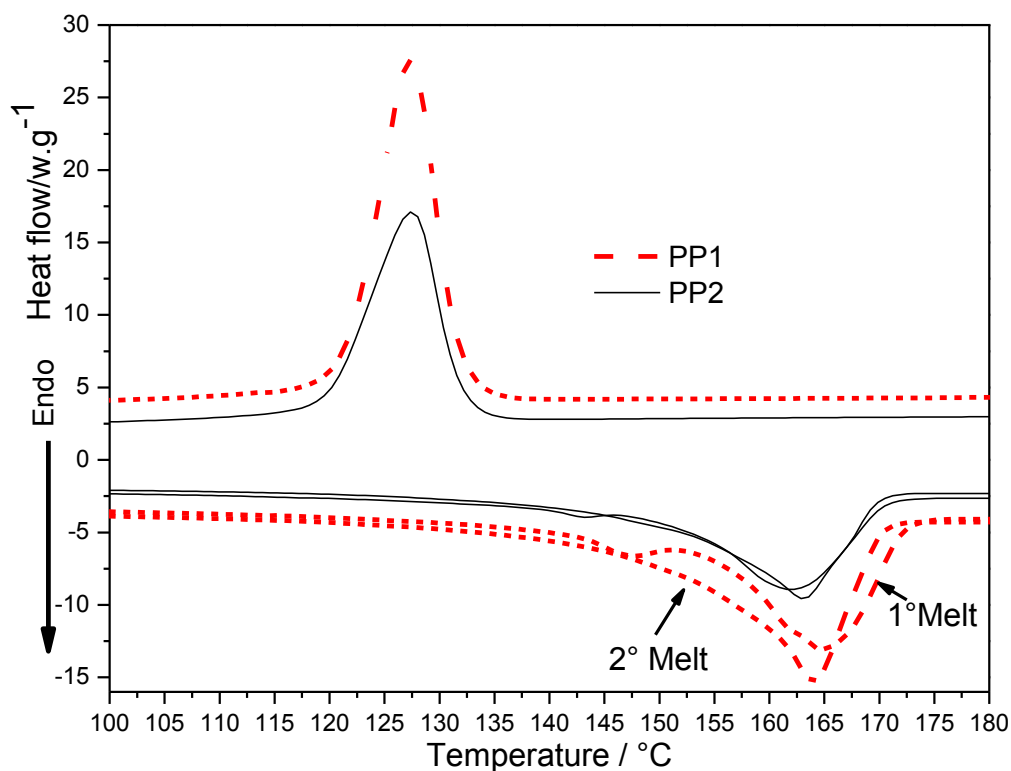


Figure 5: DSC curves of PP1 and PP2 nanocomposite.

Crystallization was affected by clay addition since nanoclays serve as nucleating agents. In consequence of clay content, the crystallinity should be higher. As shown in Table 1 the value of the crystallinity of the PP film is much larger than that nanocomposite film PP2. The question is why this occurred. An possible explanation was reported by Waldman [28] and Ataefard [29] in research of the polypropylene with MMT. Results after the two heating cycles processes show that the nanocomposites crystallinity has a decreasing tendency as a function of higher clay content nanocomposites. This behavior can be attributed to the presence of the lamellae organoclay, which causes difficulty for the polymer chains segments to move. Furthermore, it can be noted that the crystalline melting temperature of the samples did not change with the addition of organoclay.

3.5. X-ray diffraction

In such intercalated nanocomposites, the repetitive multilayer structure is well preserved, allowing the interlayer spacing to be determined, Fig. 6.

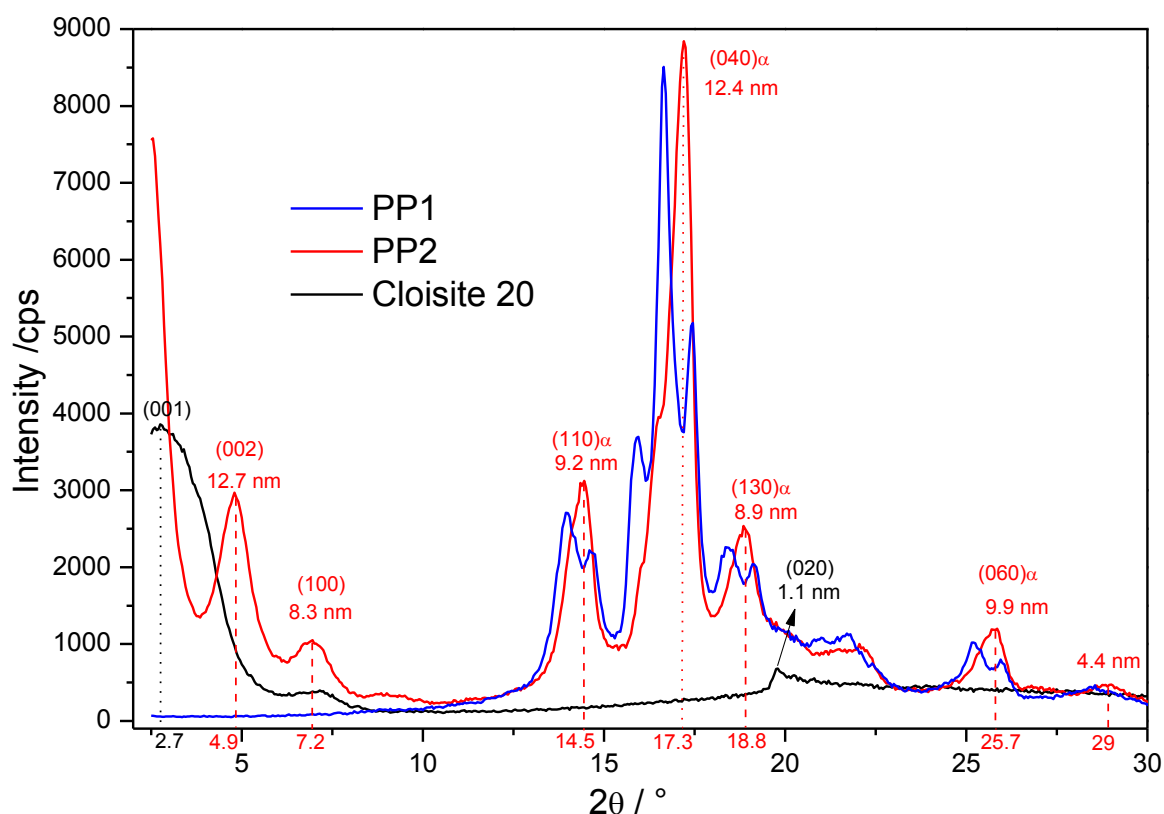


Figure 6: Typical XRD patterns from polypropylene HMSPP 12.5 kGy (PP1), polypropylene HMSPP 12.5 kGy nanocomposite (PP2), and clay Cloisite 20.

The finite layer expansion associated with the polypropylene intercalation results in the appearance of a new basal reflection corresponding to larger gallery space [30]. The sample PP2 showed intercalated and flocculated morphology. In X-rays analysis, Fig.6, diffraction peaks corresponding to interplanar distance of PP2 sample: $d_{(002)}=17.9 \text{ \AA}$, $d_{(100)}=12.2 \text{ \AA}$, $d_{(110)\alpha}=6.1 \text{ \AA}$, $d_{(040)\alpha}=5.1 \text{ \AA}$, $d_{(130)\alpha}=4.7 \text{ \AA}$, $d_{(060)\alpha}=3.4 \text{ \AA}$. The appearance of peaks in $\theta=4.9^\circ$ with crystallite 12.7 nm and $\theta=7.2^\circ$ for crystallite 8.3 nm were indicative of intercalation in the nanocomposite sample PP2.

4. CONCLUSIONS

The polypropylene nanocomposite film PP2 showed micrometric Clay aggregates. Larger particles were observed and attributed to inhomogeneous dispersion of Clay in polypropylene matrix, as well as, in X-ray patterns indicated que the polymer chains were intercalated between Clay platelets, whereas no evidence of exfoliation was found. We can explore as the results obtained, the processing of the composite materials was not sufficient to exfoliation of Clay and this factor contributed to the heterogeneity of the system and also hinders the dispersion of the silver-particles. The crystallization was affected by Clay addition since nanoclay serve in principle, as nucleation agents. The characterized, the value of the PP film crystallinity is larger than that of nanocomposite film PP2. This behavior can be attributed to the presence of the lamellae organoclay which causes polymer chains segments difficulty to move. The films PP2 did not show efficiency to combat the bacteria *E. coli* and *S. aureus*, therefore, our challenge for future work.

ACKNOWLEDGEMENTS

The authors acknowledge financial support for this work from CAPES, CNPQ. Centre of Science and Technology of Materials – CCTM/IPEN, for microscopy analysis (SEM), the technicians Mr. Eleosmar Gasparin and Nelson R. Bueno, for technical support and multipurpose gamma irradiation facility at the CTR/IPEN.

REFERENCES

1. A. Bouaziz, M. Jaziri, F. Dalmas, V. Massardier, “Nanocomposites of silica reinforced polypropylene: Correlation Between morphology and properties,” *Polymer Engineering Science*, **54**, pp. 2187-2196 (2014).
2. *Radiation processing of polymer materials and its industrial applications*. Chapter 8 – Long chain branching of polymer resins. Makuuchi, Keizo and Cheng, Song, John Wiley & Sons, INC, New Jersey – EUA, p. 248-275, 2012.
3. K. Cao, Y. Li, Z. Q. Lu, S. L. Wu, Z. H. Chen, Z. Y., Z. M. Huang, “Preparation and Characterization of High Melt Strength Polypropylene with Long Chain Branched Structure by the Reactive Extrusion Process,” *Journal of Applied Polymer Science*, **121**, pp. 3384–3392 (2011).
4. M. Rätzsch, M. Arnold, E. Borsig, H. Bucka, N. Reichelt, “Radical reactions on polypropylene in the solid state,” *Progress Polymer Science*, **27**, pp. 1195-1282 (2002).
5. W. L. Oliani, L. F. C. P. Lima, D. F. Parra, D. B. Dias, A. B. Lugao, “Study of the morphology, thermal and mechanical properties of irradiated isotactic polypropylene films,” *Radiation Physics Chemistry*, **79**, pp. 325 (2010).
6. N. Perkas, M. Shuster, G. Amirian, Y. Koltypin, A. Gedanken, “Sonochemical Immobilization of Silver Nanoparticles on Porous Polypropylene,” *Journal Polymer Science Part A: Polymer Chemistry*, **46**, pp. 1719–1729 (2008).
7. M. J. Hanus, A. T. Harris, “Nanotechnology innovations for the construction industry,” *Progress Material Science*, **58**, pp. 1056–1102 (2013).
8. T. Domenech, E. P. Disdier, B. Vergnes, “The importance of specific mechanical energy during twin screw extrusion of organoclay based polypropylene nanocomposites,” *Composites Science and Technology*, **75**, pp. 7–14 (2013).
9. *Antimicrobial Polymers*. Edited by José M. Lagarón, María J. Ocio, Amparo López-Rubio. Chapter 13 – Nanometals as antimicrobials. R.P. Allaker, M.A. Vargas-Reus, G.G. Ren. John Wiley & Sons, New Jersey-EUA. 327-345, 2012.
10. M. Modesti, A. Lorenzetti, D. Bon, S. Besco, “Effect of processing conditions on morphology and mechanical properties of compatibilized polypropylene nanocomposites,” *Polymer*, **46**, pp. 10237–10245 (2005).
11. S. Hotta, D. R. Paul, “Nanocomposites formed from linear low density polyethylene and organoclays,” *Polymer*, **45**, pp. 7639–7654 (2004).
12. J. H. Bang, K. S. Suslick, “Applications of Ultrasound to the Synthesis of Nanostructured Materials,” *Advanced Materials*, **22**, pp. 1039–1059 (2010).
13. S. J. C., B. Zou, F. Collins, X. L. Zhao, M. Majumber, W. H. Duan, “Predicting the influence of ultrasonication energy on the reinforcing efficiency of carbon nanotube,” *Carbon*, pp.1-10 (2014).
14. A.I. Isayev, R. Kumar, T. M. Lewis, “Ultrasound assisted twin screw extrusion of polymer–nanocomposites containing carbon nanotubes,” *Polymer*, **50**, pp. 250–260 (2009).

15. R. Foldbjerg, P. Olesen, M. Hougaard, D. A. Dang, H. J. Hoffmann, H. Autrup, "PVP coated silver nanoparticles and silver ions induce reactive oxygen species, apoptosis and necrosis in THP-1 monocytes," *Toxicology Letters*, **28**, 190(2), pp. 156-62 (2009).
16. M. I. Azo'car, L. Tamayo, N. Vejar, G. Gómez, X. Zhou, G. Thompsom, E. Cerda, M. J. Kogan, E. Salas, M. A. Paez, "A systematic study of antibacterial silver nanoparticles: efficiency, enhanced permeability, and cytotoxic effects," *Journal of Nanoparticle Research*, **16**, pp.2465 (2014).
17. W. L. Oliani, D. F. Parra, L. F. C. P. Lima, A. B. Lugao, "Morphological characterization of branched PP under stretching," *Polymer Bulletin*, **68**, pp.2121–2130 (2012).
18. W. L. Oliani, D. F. Parra, A. B. Lugao, "UV stability of HMS-PP (high melt strength polypropylene) obtained by radiation process," *Radiation Physics Chemistry*, **79**, pp.383 (2010).
19. JIS Z 2801:2010 (adapted). Japanese Industrial Standard. Antimicrobial Products - Test for antimicrobial activity and efficacy.
20. J. G. M. Colunga, S. S. Valdes, L. F. R.Valle, L. M. Jimenez, E. R. Vargas, M. C. I. Alonso, T. L. Ramirez, P. G. Lafleur, "Simultaneous Polypropylene Functionalization and Nanoclay Dispersion in PP/Clay Nanocomposites using Ultrasound," *Journal of Applied Polymer Science*, **131**, pp. 40631 (2014).
21. T. Li, S. Xiang, P. Ma, H. Bai, W. Dong, M. Chen, "Nanocomposite Hydrogel Consisting of Na-montmorillonite with Enhanced Mechanical Properties," *Journal of Polymer Science Part B: Polymer Physics*, DOI: 10.1002/polb.23732 (2015).
22. E. V. D. G. Líbano, L. L. Y. Visconte, E. B. A. V. Pacheco, "Propriedades térmicas de compósitos de polipropileno e bentonita organofílica," *Polímeros*, **22**, 5, pp.430-435 (2012).
23. C. D. Angel, A. B. Morales, F. N. Pardo, T. Lozano, P. G. Lafleur, S. S. Valdes, G. M. Colunga, E. R. Vargas, S. Alonso, R. Zitzumbo, "Mechanical and rheological properties of polypropylene/bentonite composites with stearic acid as an interface modifier," *Journal of Applied Polymer Science*, pp.42264 (2015).
24. P. A. Zapata, L. T., M. Paez, E. Cerda, I. Azocar, F. M. Rabagliati, "Nanocomposites based on polyethylene and nanosilver particles produced by metalocenic "in situ" polymerization: synthesis, characterization, and antimicrobial behavior," *European Polymer Journal*, **47**, pp. 1541–1549 (2011).
25. F. C. Morelli, A. R. Filho, "Nanocompósitos de polipropileno e argila organofílica: Difração de raios-x, espectroscopia de absorção na região do infravermelho e permeação ao vapor d'água," *Polímeros*, **20**, pp.121-125 (2010).
26. G. Lee, C. K. Kim, M. K. Lee, C. K. Rhee, "Facile synthesis of surface oxide free copper nanoparticles by in-situ coating with oleic acid," *Powder Technology*, **261**, pp. 143–146 (2014).
27. C. P. F. Santos, D. M. A. Melo, A. A. F. Melo, E. V., Sobrinho, "Characterization and uses of bentonite and vermiculite clays for absorption of copper (II) in solution," *Cerâmica*, **48**, pp. 178-182 (2002).
28. L. B. Fitaroni, J. A. Lima, S. A. Cruz, W. R. Waldman, "Thermal stability of polypropylene-montmorillonite clay nanocomposites: Limitation of the Thermogravimetric analysis," *Polymer Degradation and Stability*, **111**, pp.102-108 (2015).
29. M. Ataefard, S. Moradian, "Polypropylene/organoclay nanocomposites: effects of clay content on properties," *Polymer Plastic Technology Engineering*, **50**, pp.732-739 (2011).
30. S. S. Ray, M. Okamoto, "Polymer/layered silicate nanocomposites: a review from preparation to processing," *Progress Polymer Science*, **28**, pp.1539–641 (2003).